Binding Modes of Distamycin A with d(CGCAAATTTGCG)$_2$ Determined by Two-Dimensional NMR

Jeffrey G. Pelton and David E. Wemmer*

Contribution from the Department of Chemistry, University of California, and Chemical Biodynamics Division, Lawrence Berkeley Laboratory, 1 Cyclotron Road, Berkeley, California 94720. *Received June 21, 1989*

Abstract: Two-dimensional nuclear Overhauser effect spectroscopy (NOESY) was used to study the interaction of distamycin A with d(CGCAAATTTGCG)$_2$. Spectra acquired at several points in a titration of the dodecamer with distamycin A were used to assign resonances, to determine drug-drug and drug-DNA contact points, and to monitor exchange of the drug between binding sites. At low drug:DNA ratios (0.5 equiv), both one-drug and symmetric two-drug binding modes were observed, while at high ratios (2 equiv), the two-drug complex was the primary species present. The off-rate for the drug from the 2:1 mode was found to be slow on the NMR time scale (0.2 ± 0.1 s^{-1}, 30 °C), facilitating characterization of the distamycin A binding sites in this mode. NOEs from drug pyrrole H3 to DNA C1'H and adenine C2H protons, as well as observed line width changes of the DNA protons as a function of temperature, were consistent with a model in which two drugs bind simultaneously, overlapping in the minor groove, with each drug sliding between 5'-AATT-3' and 5'-ATTT-3' binding sites at a rate fast on the NMR time scale. Molecular modeling of the 2:1 complexes indicates that the minor groove must expand, relative to the 1:1 complex, to accommodate both drugs, indicating that the phosphate backbone can be distorted in response to ligand binding. Distance-constrained energy refinement of the 2:1 complexes indicates that electrostatic interactions, hydrogen bonds between the drugs and the DNA, and both drug-drug and drug-DNA stacking interactions all contribute to stabilization of the complex. Comparisons are made with crystallographic studies of this drug and dodecamer. Implications of the 2:1 binding mode for other studies and possibilities for the design of new sequence-specific recognition complexes are discussed.

Distamycin A is an oligopeptide antibiotic that inhibits binding of RNA polymerase, and hence transcription in vitro,[1] by binding to the minor groove of A-T-rich initiation sites.[2] The complexes formed between this drug and various DNA oligomers have been used as model systems for the investigation of sequence-specific recognition and have thus been the subject of much study. In particular, structural investigations of distamycin A-DNA complexes have aimed at understanding the possible binding modes, sequence specificity, and forces responsible for drug binding, while kinetic investigations have aimed at understanding how the drug exchanges between the possible binding modes. Information obtained from such studies should aid in the design of new drugs and should also provide insight into both DNA conformational flexibility and protein-DNA interactions.

Many techniques have been used to study the binding of distamycin A, and the related drug netropsin, to DNA, sometimes with contradictory results. Preferred sequences for the binding of the drug have been identified by footprinting and affinity cleaving studies.[3] This work showed that the drug covers five base pairs and that it binds preferentially to 5'-AAATT-3' and, in general, prefers poly(dA)·poly(dT) sites. Calorimetric studies[4] also indicate strong binding to the polymers poly(dA)·poly(dT) and poly[d(A-T)]·poly[d(A-T)]. NMR studies[5] of distamycin A with d(CGCGAATTCGCG)$_2$ indicated that the minimal binding site consists of just four A-T base pairs. Subsequent calorimetric studies[4] have shown that distamycin A binds tightly to the four-base site 5'-AATT-3' within the sequence d-(GCGAATTCGC)$_2$, with a binding constant of 2.7×10^8 M^{-1}. This is in striking contrast to the binding constant of 2×10^5 M^{-1} reported for the 5'-TATA-3' site within the sequence d(GGTA-TACC)$_2$,[6] obtained by quantitative analysis of footprinting data, showing that the drug displays a high degree of A-T sequence specificity, although the reasons for this remain unclear. More recent NMR studies of distamycin A with d-(CGCAAATTGGC):d(GCCAATTTGCG)[7] have revealed at low drug to DNA ratios (<1.0) that the drug binds to several different sites containing four base pairs. In addition, a new binding mode was observed near and above 1 equiv of added drug, in which two distamycin A molecules bound simultaneously, overlapping in the minor groove of the undecamer. In contrast, a recent crystallographic study[8] of distamycin A with the symmetric dodecamer d(CGCAAATTTGCG)$_2$ revealed that the drug bound to only one site, namely 5'-ATTT-3', although other sides were available. On the basis of these and similar studies with netropsin[9] and Hoechst 33258,[10] van der Waals contacts, hydrogen bonds, and electrostatic forces[11] have been proposed to account for the sequence specificity

* Address correspondence to this author at the Department of Chemistry, University of California, Berkeley, CA 94720.

(1) Puschendorf, B.; Petersen, E.; Wolf, H.; Werchau, H.; Grunicke, H. *Biochim. Biophys. Res. Commun.* **1971**, *43*, 617-624.

(2) For reviews see: (a) Hahn, F. E. In *Antibiotics III. Mechanism of Action of Antimicrobial and Antitumor Agents*; Corcoran, J. W., Hahn, F. E. Eds.; Springer-Verlag: New York, 1975; pp 79-100. (b) Zimmer, C.; Wahnert, U. *Prog. Biophys. Mol. Biol.* **1986**, *47*, 31-112.

(3) Schultz, P. G.; Dervan, P. B. *J. Biomol. Struct. Dyn.* **1984**, *1*, 1133-1147.

(4) Breslauer, K. J.; Remeta, D. P.; Chou, W.-Y.; Ferrante, R.; Curry, J.; Zaunczkowski, D.; Snyder, J. G.; Marky, L. A. *Proc. Natl. Acad. Sci. U.S.A.* **1987**, *84*, 8922-8926.

(5) (a) Klevit, R. E.; Wemmer, D. E.; Reid, B. R. *Biochemistry* **1986**, *25*, 3296-3303. (b) Pelton, J. G.; Wemmer, D. E. *Biochemistry* **1988**, *27*, 8088-8096.

(6) Fish, L.; Lane, M. J.; Vournakis, J. N. *Biochemistry* **1988**, *27*, 6026-6032.

(7) (a) Pelton, J. G.; Wemmer, D. E. In *Frontiers of NMR in Molecular Biology*; Live, D., Armitage, I., Patel, D. Eds.; UCLA Symposia on Molecular and Cellular Biology, New Series; Alan R. Liss Inc.: New York, 1989; in press. (b) Pelton, J. G.; Wemmer, D. E. *Proc. Natl. Acad. Sci. U.S.A.* **1989**, *86*, 5723-5727.

(8) Coll, M.; Frederick, C. A.; Wang, A. H.-J.; Rich, A. *Proc. Natl. Acad. Sci. U.S.A.* **1987**, *84*, 8385-8389.

(9) (a) Patel, D. J. *Proc. Natl. Acad. Sci. U.S.A.* **1982**, *79*, 6424-6428. (b) Pardi, A.; Morden, D. M.; Patel, D. J.; Tinoco, I. *J. Am. Chem. Soc.* **1983**, *22*, 1107-1113. (c) Sarma, M. H.; Gupta, G.; Sarma, R. H. *J. Biomol. Struct. Dyn.* **1985**, *2*, 1085-1095. (d) Patel, D. J.; Shapiro, L. *Biochimie* **1985**, *67*, 887-915. (e) Kopka, M. L.; Yoon, C.; Goodsell, D.; Pjura, P.; Dickerson, R. E. *Proc. Natl. Acad. Sci. U.S.A.* **1985**, *82*, 1376-1380. (f) Kopka, M. L.; Yoon, C.; Goodsell, D.; Pjura, P.; Dickerson, R. E. *J. Mol. Biol.* **1985**, *183*, 553-563. (g) Kopka, M. L.; Pjura, P.; Yoon, C.; Goodsell, D.; Dickerson, R. E. In *Structure and Motion: Membranes, Nucleic Acids, and Proteins*; Clementi, E., Corongiu, G., Sarma, M. H., Sarma, R. H., Eds.; Adenine Press: New York, 1985; pp 461-483. (h) Patel, D. J.; Shapiro, L. *J. Biol. Chem.* **1986**, *261*, 1230-1239. (i) Coll, M.; Aymami, J.; van der Marel, G. A.; van Boom, J. H.; Rich, A.; Wang, A. H.-J. *Biochemistry* **1989**, *28*, 310-320. (j) Ward, B.; Rehfuss, R.; Goodisman, J.; Dabrowiak, J. C. *Biochemistry* **1988**, *27*, 1198-1205. (k) Caldwell, J.; Kollman, P. *Biopolymers* **1986**, *25*, 249-266. (l) Zakrzewska, K.; Lavery, R.; Pullman, B. *Nucleic Acids Res.* **1983**, *11*, 8825-8839.

(10) (a) Pjura, P. E.; Grzeskowiak, K.; Dickerson, R. E. *J. Mol. Biol.* **1987**, *197*, 257-271. (b) Teng, M.-K.; Usman, N.; Frederick, C. A.; Wang, A. H.-J. *Nucleic Acids Res.* **1988**, *16*, 2671-2690.

0002-7863/90/1512-1393$02.50/0

of the drug and the stability of its complexes with DNA.

In addition to the emerging structural picture of these complexes, drugs of this general class have been shown to undergo several dynamical processes. For instance, NMR studies of the 2:1 distamycin A–d(CGCAAATTGGC):d(GCCAATTTGCG) complex have shown that the off-rate for the drug was on the order of 2–4 s^{-1},[7a] similar to the off-rate for the drug in the 1:1 complex with $d(CGCGAATTCGCG)_2$,[5a] about 4 s^{-1}. Distamycin A was also shown to exchange between two symmetrically related binding sites on $d(CGCGAATTCGCG)_2$ by a "flip-flop" mechanism,[5a] with a rate constant near 2 s^{-1}. The minor-groove-binding drugs netropsin,[9d,h] a netropsin analogue,[12] (4*S*)-(+)- and (4*R*)-(−)-anthelvencin A,[13] and a bis(quanternary ammonium) heterocycle, SN6999,[14] have also been shown to exchange between two symmetrically related binding sites on their respective DNA sequences, indicating that such a process is a common feature of these minor-groove-binding drugs.

We expected, on the basis of our studies of distamycin A with $d(CGCGAATTCGCG)_2$[5] and d(CGCAAATTGGC):d(GCCAATTTGCG) (A_3T_2 duplex),[7] that the sequence $d(CGCAAATTTGCG)_2$ (A_3T_3 duplex) would contain several good distamycin A binding sites and might also contain a two-drug site analogous to that seen for the A_3T_2 duplex, in contrast to the crystallographic result. We have therefore undertaken an investigation of this system using nuclear Overhauser effect spectroscopy (NOESY)[15] in order to determine the binding modes present and to probe the dynamics of the drug exchange between these modes in solution. Semiquantitative distance constraints derived from NOESY spectra were used in conjunction with the assisted model building and energy refinement (AMBER)[16] molecular mechanics program to generate structures of the 2:1 complexes. These structures were analyzed to identify those interactions that might be responsible for stabilization of each complex.

Materials and Methods

Distamycin A [B-[1-methyl-4-[1-methyl-4-[1-methyl-4-(formylamino)pyrrole-2-carboxamido]pyrrole-2-carboxamido]pyrrole-2-carboxamido]propionamidine] was purchased from Sigma and used without further purification. Drug concentrations were determined optically with an extinction coefficient of 34 000 M^{-1} cm^{-1} at 303 nm. Due to its instability in aqueous solution, fresh samples were prepared for each titration. The self-complementary oligomer d(CGCAAATTTGCG) was synthesized and purified as described previously.[7b] The extinction coefficient for the sequence was calculated[17] to be 1.125×10^5 M^{-1} cm^{-1}. Absorbances were determined at 80 °C. Double-strand DNA concentrations used in the various experiments ranged from 1 to 4 mM, in buffer consisting of 10 mM sodium phosphate (pH 7.0) and 10 mM sodium chloride.

NOESY spectra were acquired on a GN-500 spectrometer (General Electric Instruments) at drug:DNA ratios of 0.5:1 (30 °C) and 2:1 (20, 50 °C) and were processed as described.[5b] All NOESY experiments were performed with a 150-ms mixing period. For each t_1, 64 scans were signal-averaged, taking 1024 complex points with a recycle time of 2.2 s; 400–512 t_1s were recorded per experiment. A spectral width of 5000 Hz resulted in a digital resolution of 4.9 Hz/point. One-dimensional NOE difference spectra of exchangeable protons were acquired by interleaving on- and off-resonance saturated spectra. A 1-3-3-1 pulse sequence[18] was used to suppress the solvent resonance.

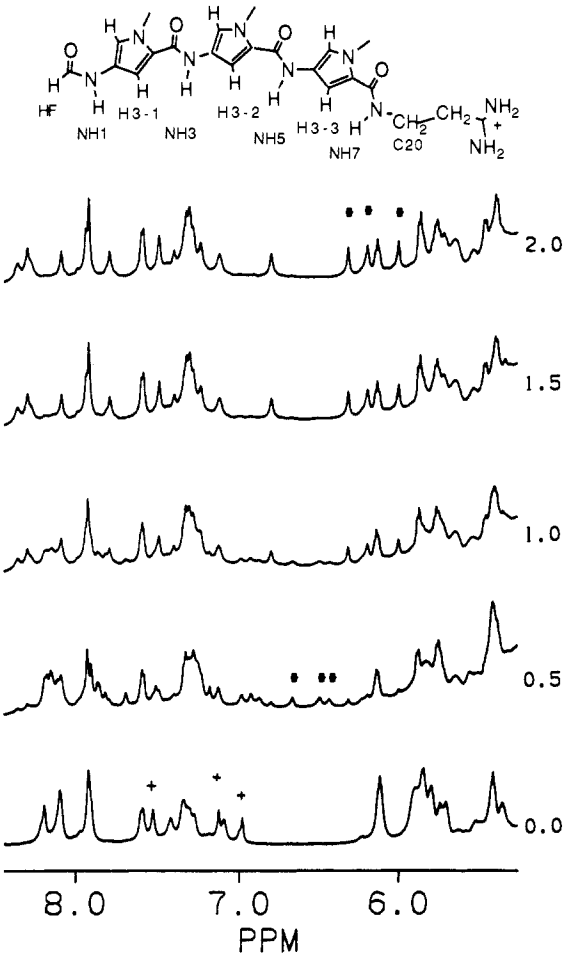

Figure 1. (Top) Schematic of distamycin A. It consists of a formyl group, followed by three *N*-methylpyrrole carboxamide units, and a propylamidinium group. (Bottom) Aromatic and C1′H regions of NMR spectra acquired at several points in a titration of $d(CGCAAATTTGCG)_2$ with distamycin A (35 °C). The three upfield H3 pyrrole proton chemical shifts (two-drug mode) are indicated by the right-most asterisks. The three downfield pyrrole H3 protons (one-drug mode) are indicated by the left-most asterisks. Plus signs denote the chemical shifts of the three adenine C2H resonances of the uncomplexed dodecamer.

Results

Titration of the A_3T_3 Duplex with Distamycin A. Spectra obtained at several points in a titration of the A_3T_3 duplex with distamycin A are presented in Figure 1. After the initial addition of drug, the spectra are quite complex due to the appearance of many new resonances, as well as the broadening and the reduced intensity of resonances belonging to the free duplex. Six new resonances appear between 6.0 and 6.7 ppm, characteristic of the drug H3 pyrrole protons, while the A4, A5 and A6 C2H resonances of the free duplex that resonate at 7.11, 7.00, and 7.53 ppm,[19] respectively (Table I), become significantly broader and reduced in intensity. Upon further drug additions, the upfield set of H3 pyrrole resonances at 6.02, 6.20, and 6.34 ppm and also several peaks near 8.3 ppm grow in intensity, while the other set of H3 resonances at 6.44, 6.50, and 6.67 ppm begins to diminish. This trend continues until the downfield set of H3 resonances essentially disappears (1.5 equiv) and growth of the upfield set of H3 resonances stops (2.0 equiv). At this point, DNA resonances corresponding to only one strand of the A_3T_3 duplex are observed,

(11) (a) Zakrezewska, K.; Lavery, R.; Pullman, B. *J. Biomol. Struct. Dyn.* **1987**, *4*, 833–843. (b) Lavery, R.; Pullman, A.; Pullman, B. *Theor. Chim. Acta* **1982**, *62*, 93–106.

(12) (a) Second pyrrole ring of netropsin replaced by an imidazole ring. (b) Lee, M.; Chang, D.-K.; Hartley, J. A.; Pon, R. T.; Krowicki, K.; Lown, J. W. *Biochemistry* **1988**, *27*, 445–455.

(13) Lee, M.; Shea, R. G.; Hartley, S. A.; Kissinger, K.; Pon, R. T.; Vesnaver, G.; Breslauer, K. J.; Dabrowick, J. C.; Lown, J. W. *J. Am. Chem. Soc.* **1989**, *111*, 345–354.

(14) Leupin, W.; Chazin, W. J.; Hyberts, S.; Denny, W. A.; Wuthrick, K. *Biochemistry* **1986**, *25*, 5902–5910.

(15) Jeener, J.; Meier, B. H.; Bachmann, P.; Ernst, R. R. *J. Chem. Phys.* **1979**, *71*, 4546–4553.

(16) Weiner, S. J.; Kollman, P. A.; Case, D. A.; Singh, U. C.; Ghio, C.; Alagona, G.; Profeta, S., Jr.; Weiner, P. *J. Am. Chem. Soc.* **1984**, *106*, 765–784.

(17) Warshaw, M.; Cantor, C. *Biopolymers* **1970**, *9*, 1079–1103.

(18) Hore, P. J. *J. Magn. Reson.* **1983**, *55*, 283–300.

(19) (a) Numbering scheme for the symmetric A_3T_3 duplex is 5′ to 3′, residues 1–12. (b) Assigned by standard methods, see: (c) Feigon, J.; Leupin, W.; Denny, W. A.; Kearns, D. R. *Biochemistry* **1983**, *22*, 5930–5942. (d) Scheek, R. M.; Boelens, R.; Russo, W.; van Boom, J. H.; Kaptein, R. *Biochemistry* **1984**, *23*, 1371–1376. (e) Hare, D. R.; Wemmer, D. E.; Chou, S.-H.; Drobny, G.; Reid, B. R. *J. Mol. Biol.* **1983**, *171*, 319–336.

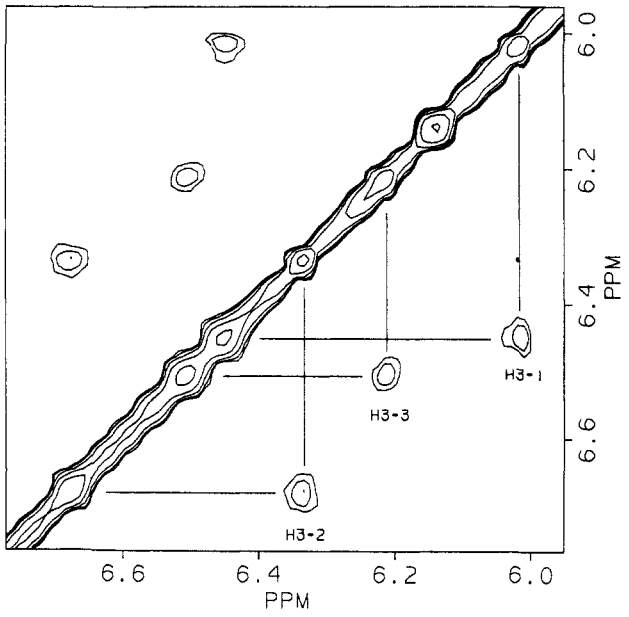

Figure 2. Expansion of a NOESY/exchange spectrum of the A_3T_3 duplex acquired after addition of 0.5 equiv of distamycin A (30 °C, 150 ms). The downfield and upfield sets of H3 resonances correspond to the one-drug and two-drug binding modes, respectively. The cross peaks arise from chemical exchange of the drug between binding modes.

suggesting the formation of a symmetric 2:1 drug:DNA complex. Further additions of drug cause resonances from free drug H3 and H5 pyrrole protons to appear at 6.58 and 6.49 ppm, respectively, indicating that the drug binding sites had become saturated.

The initial appearance and then disappearance of the downfield set of H3 resonances, combined with the appearance of a set of upfield H3 resonances, which then grew in intensity until 2 equiv of drug had been added, suggest that it is possible for distamycin A to bind in both one-drug and symmetric two-drug modes. From the intensities of the H3 resonances associated with both of these modes, it was found that the binding constant for binding of the second drug was larger than the binding constant for binding of the first drug by a factor of approximately 1.7. To investigate whether we could detect exchange of the drug between these binding modes, we acquired a NOESY spectrum of the duplex at a relatively low drug:DNA ratio (0.5 equiv) where both binding modes were populated (Figure 2). In this spectrum cross peaks correlate the upfield and downfield sets of H3 resonances. These cross peaks are due to exchange and arise when a drug initially in one binding mode has transferred to the other mode during the mixing time. From the intensities of the exchange cross peaks and the diagonal peaks associated with the two-drug mode, we calculate the off-rate for the drug from the 2:1 complex to be 0.2 $\pm$ 0.1 s^{-1} at 30 °C. A more accurate determination would require an analysis of the time dependence of the cross and diagonal peak intensities in order to account for both longitudinal and cross-relaxation effects,[15] which was not attempted.

For the one-drug binding mode, the fact that only one set of H3 resonances is seen suggests either that distamycin A binds to only one site, as observed in the crystal structure of the drug with the A_3T_3 duplex,[8] or that the drug is in fast exchange among several binding sites. In the latter case the drug H3 protons would resonate at population-weighted average chemical shifts. The behavior seen in the 2:1 mode (see below) suggests that such dynamic averaging may well occur. At low drug concentrations, where the one-drug mode is significantly populated, a complex mixture of species is present in solution, precluding a structural characterization of the 1:1 binding site(s). At high drug concentrations, however, the 2:1 complex is the primary species present, facilitating assignment and structural characterization of this complex, which will be discussed presently.

Assignment of Resonances in the 2:1 Complex. Expansions of the aromatic to upfield (1.0 ppm) and aromatic to C1′H regions

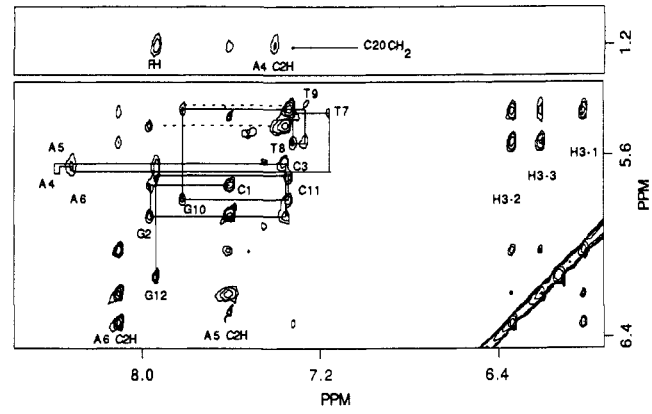

Figure 3. Expansions of the aromatic to upfield and aromatic to C1′H regions of a NOESY spectrum of the 2:1 distamycin A–d(CGCAAATTTGCG)$_2$ complex (20 °C, 150 ms). Sequential connectivities are denoted by solid lines. Intraresidue aromatic to C1′H cross peaks are indicated with numbers. Drug proton and DNA C2H proton chemical shifts are explicitly labeled. Dashed lines denote cytosine C5H to aromatic proton connectivities. Peaks labeled with an X, which were also observed in NOESY spectra of the free duplex, result from oligonucleotide impurities and represent less than 10% of the total DNA concentration.

of a NOESY spectrum of the 2:1 complex are presented in Figure 3. This spectrum contains both intramolecular NOEs used to assign DNA resonances and intermolecular NOEs used to identify drug–DNA contact points. The DNA aromatic and C1′H protons can be assigned from NOESY spectra by observation of sequential NOEs between an aromatic proton and both its own C1′H and the C1′H of its 5′ neighbor as described.[19c-e] For the A_3T_3 duplex with 2 equiv of added drug, sequential connectivities can be traced from C1 to C3 and from T7 to G12. However, the aromatic to C1′H cross peaks associated with A4, A5, and A6 either are missing or are ambiguous. Analysis of the aromatic to C2′H/C2″H/CH_3 region of this spectrum (not shown) revealed cross peaks between C3 C2′H/C2″H and A4 H8 and between A6 H8 and T7 CH_3, which were used to identify the A4 and A6 H8 chemical shifts. Given these assignments, it was clear from the aromatic to C2′H/C2″H NOEs associated with the three adenine residues that A5 H8 resonates at 8.34 ppm.

One-dimensional spectra of the A_3T_3 duplex with 2 equiv of drug at various temperatures were collected (supplementary material). As the temperature is reduced from 55 to 5 °C, there is a general broadening of the resonances, with several peaks, including both the aromatic and C1′H resonances of A4, A5, and A6, broadening more than the other aromatic and C1′H peaks. This differential line broadening is indicative of an exchange process that is intermediate on the NMR time scale, whereby the line width of a particular resonance is dependent on the chemical shift difference of the proton in its various binding sites and the rate of exchange.

We reasoned that the adenine aromatic to C1′H cross peaks in the NOESY spectrum acquired at 20 °C (Figure 3) were weak because of exchange broadening and therefore acquired a NOESY spectrum of the 2:1 complex at 50 °C, where these resonances were better resolved. In this spectrum (not shown) all of the aromatic to C1′H cross peaks were weak, and, in particular, the interresidue C3 C1′H to A4 H8 and intraresidue A6 H8 to C1′H cross peaks were not visible. However, the sequential connectivities could be traced unambiguously in the aromatic to C2′H/C2″H region (supplementary material), confirming the A4, A5, and A6 H8 assignments. Given the C2′H/C2″H assignments, it was then possible, with aromatic–C2′H/C2″H–C1′H cross peaks, to assign each of the adenine C1′H peaks. The fact that resonances corresponding to only one strand of the duplex were observed after the addition of 2 equiv of drug indicates that the DNA in the complex is symmetric, showing that the drugs must bind in a symmetric fashion. Moreover, a review of the intensities of the observed intra- and interresidue DNA cross peaks in both NOESY spectra did not suggest any striking conformational changes to

Table I. Chemical Shift Assignments of the A_3T_3 Duplex (ppm)

DNA proton	free duplex	two-drug complex	diff
C1 H6	7.61	7.60	−0.01
C1 C1'H	5.71	5.73	0.02
G2 H8	7.93	7.96	0.03
G2 C1'H	5.84	5.86	0.02
C3 H6	7.31	7.35	0.04
C3 C1'H	5.31	5.63	0.32
A4 H8	8.21	8.38	0.17
A4 C1'H	5.75	5.70	−0.05
A4 C2H	7.11	7.40	0.29
A5 H8	8.11	8.34	0.23
A5 C1'H	5.88	5.66	−0.22
A5 C2H	7.00	7.61	0.61
A6 H8	8.10	8.30	0.20
A6 C1'H	6.12	5.73	−0.39
A6 C2H	7.53	8.10	0.57
T7 H6	7.12	7.16	0.04
T7 C1'H	5.90	5.40	−0.50
T8 H6	7.43	7.32	−0.11
T8 C1'H	6.11	5.54	−0.57
T9 H6	7.28	7.27	−0.01
T9 C1'H	5.85	5.39	−0.46
G10 H8	7.91	7.81	−0.10
G10 C1'H	5.78	5.79	0.01
C11 H6	7.36	7.34	−0.02
C11 C1'H	5.73	5.69	−0.04
G12 H8	7.94	7.93	−0.01
G12 C1'H	6.12	6.13	0.01

the A_3T_3 duplex upon drug binding. A more quantitative analysis was not attempted because of complications due to exchange of the drug between binding sites (see below) during the NOESY mixing period.

The adenine C2H resonances were assigned with use of both the NOESY spectrum[20] of Figure 3 and sequential one-dimensional NOEs of the DNA imino protons[21] (supplementary material). The DNA aromatic and C1'H proton assignments of the A_3T_3 duplex alone and with 2 equiv of drug are summarized in Table I, together with the change in chemical shift upon complex formation. Drug H3 resonances were assigned by observation of NOEs to these protons from drug amides (8–11 ppm) as described.[5a] The presence of two drugs in the minor groove complicated assignment of the drug aromatic protons, since both intra- and intermolecular NOEs between amide and H3 protons are possible. For this reason, we were initially unable to specifically assign H3-2 and H3-3 to either 6.20 to 6.34 ppm; H3-1 was unambiguous at 6.02 ppm. However, when the intermolecular contacts below were examined, it became clear that H3-2 must resonate at 6.34 ppm and H3-3 at 6.20 ppm to be consistent with all of the observed NOEs. In addition, our study of the 2:1 distamycin A–A_3T_2 complex[7] showed that the nonequivalent H3-3 protons were found to resonate downfield of the H3-1 protons and upfield of the H3-2 protons, consisted with our assignment here.

Intermolecular Contacts. The NOESY spectrum of the 2:1 complex (Figure 3) contains many intermolecular drug:DNA NOEs, in addition to the intramolecular ones, that can be used to identify contact points between these molecules. In particular, NOEs are observed between A5 C2H and both H3-1 and H3-3 (with the assignments as above) and between A6 C2H and each of the H3 protons. If the H3-2 and H3-3 assignments were reversed, then an NOE would be expected between H3-1 or H3-3 and A4 C2H, but no such NOE is seen, confirming our assignments. Intermolecular NOEs are also observed in this spectrum between both A4 and A5 C2H and a pair of resonances at 1.19 and 2.18 ppm, which must be the geminal C20 protons of the drug in this complex, as in the A_3T_2 complex.[7]

Table II. Intermolecular Drug–DNA and Drug–Drug Contacts

drug proton	DNA and drug protons
FH	A5 C1'H, A6 C1'H
H3-1	A5 C2H, A6 C2H, T7 and/or T9 C1'H H3-2, H3-3
H3-2	A6 C2H, T7 and/or T9 C1'H, T8 C1'H H3-1, H3-3
H3-3	A5 C2H, A6 C2H, T7 and/or T9 C1'H, T8 C1'H H3-1, H3-2
C20 CH_2	A5 C2H, A4 C2H, FH

Strong NOEs are also observed in Figure 3, between the drug H3 and DNA C1'H protons. Specifically, NOEs are observed between H3-1 and either T7 or T9 C1'H (too close to be resolved), and both H3-2 and H3-3 show NOEs to T8 and either T7 or T9 C1'H. There are also NOEs between the drug formyl proton and both A5 and A6 C1'H, although at the temperature at which this spectrum was acquired these peaks are poorly resolved and, consequently, the NOEs between these proton pairs are broad. At 50 °C, where these peaks are better resolved, the NOESY spectrum revealed distinct cross peaks between the formyl proton and these C1'H protons, confirming the presence of both contacts.

Finally, in Figure 3, cross peaks are observed from the drug formyl proton to resonances at 1.19 and 2.18 ppm and from each of the drug H3 protons to the other two, with the H3-1 to H3-2 cross peak significantly less intense than the others. All of these NOEs represent intermolecular drug–drug contacts, since the distances between these protons on a single drug are larger than 0.5 nm. The drug–drug and drug–DNA contact points are summarized in Table II.

Distamycin A Binding Modes in Crystallization Buffer. It was apparent that the NMR results were not consistent with the X-ray crystal structure of distamycin A with the A_3T_3 duplex derived under different solvent conditions.[8] In order to determine the effect of the crystallization buffer on the distamycin A binding modes, we acquired spectra of the A_3T_3 duplex in the crystallization buffer (20 mM sodium cacodylate (pH 6.5), 8 mM $MgCl_2$, 1 mM spermine, 10% (v/v) 2-methyl-2,4-pentanediol, 1 mM DNA, 1.1 mM distamycin A) and also in phosphate buffer (pH 7.0), using identical drug and DNA concentrations (supplementary material). The A_3T_3 duplex resonances in the crystallization buffer are broad because of an increase in viscosity associated with addition of the alcohol. Comparison of the two spectra clearly shows, however, that the 2:1 complex, as evidenced by the H3 resonances at 6.02, 6.20, and 6.34 ppm, is the primary species present under both buffer conditions.

Discussion

Spectra obtained at intermediate points in the titration of the A_3T_3 duplex with distamycin A indicate that both one-drug and two-drug binding modes occur with this sequence. Moreover, as indicated by the binding constant ratio (2:1/1:1) of approximately 1.7, binding of the second drug is slightly more favorable than binding of the first drug. This is to be compared to distamycin A binding with the A_3T_2 duplex,[7a] where the ratio of equilibrium constants (2:1/1:1) is less than 1. Thus, addition of another A–T base pair facilitates formation of the 2:1 complex relative to the one-drug complex.

The off-rate of distamycin A from the 2:1 complex was determined to be 0.2 ± 0.1 s^{-1} at 30 °C, which is 1 order of magnitude slower than for the drug in the 2:1 complex with the A_3T_2 duplex (2–4 s^{-1}, 35 °C).[7a] This reflects the fact that there are fundamental differences in the binding of distamycin A between these sequences. The kinetic parameters listed here, as well as those obtained from a thermodynamic analysis of the 2:1 binding mode, should provide needed insight into these differences.

Several models for the binding of two distamycin A molecules in the minor groove of the A_3T_3 duplex were considered in an attempt to explain both the drug–DNA and drug–drug NOEs. In order to be consistent with the data, the model must account

(20) (a) Patel, D. J.; Shapiro, L.; Kozlowski, S. A.; Gaffney, B. L.; Jones, R. A. *J. Mol. Biol.* **1986**, *188*, 677–692. (b) Weiss, M. A.; Patel, D. J.; Sauer, R. T.; Karplus, M. *Nucleic Acids Res.* **1984**, *12*, 4035–4047. (c) Behling, R. W.; Kearns, D. R. *Biochemistry* **1986**, *25*, 3335–3346. (d) Kintanar, A.; Klevit, R. E.; Reid, B. R. *Nucleic Acids Res.* **1987**, *15*, 5845–5862.

(21) Chou, S.-H.; Hare, D. R.; Wemmer, D. E.; Reid, B. R. *Biochemistry* **1983**, *22*, 3037–3041.

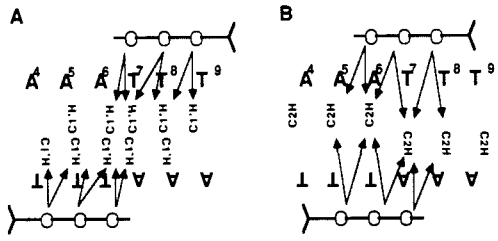

Figure 4. Schematic of models A and B considered in the binding of distamycin A to the A_3T_3 duplex. Circles represent drug pyrrole rings, and arrows indicate expected NOEs from the H3 protons. In model A, the drugs are oriented so that each of the drug H3 protons is close to two C1′H protons, consistent with the observed H3–C1′H NOEs. In model B, the drugs are oriented so that each H3 proton is close to two adenine C2H protons, consistent with the observed H3–C2H NOEs.

for the fact that A5 and A6 C2H are close to two and all three drug H3 protons, respectively, and that both H3-2 and H3-3 are close to at least two C1′H protons. In model A (Figure 4A), two drugs were placed symmetrically in the minor groove, with each pyrrole ring positioned between two base pairs so that each drug H3 proton is close to two C1′H protons. As can be seen in the figure, this model accounts for the five observed drug H3 to DNA C1′H NOEs. An NOE is also expected between H3-1 and A6 C1′H, but it is not observed experimentally. The absence of this cross peak could be due to exchange broadening, since other NOEs expected to A6 C1′H, such as the A6 H8 to C1′H NOE, were also missing. A comparison of predicted and experimentally observed drug H3 to DNA A C2H NOEs showed that this model is inconsistent with the observed NOEs between A5 C2H and H3-1 and between A6 C2H and H3-3, which have intensities that indicate distances between these proton pairs of less than 0.28 and 0.35 nm, respectively.[22] A structure of model A was generated by interactively docking distamycin A into the minor groove of the A_3T_3 duplex. In this structure, the distance between each of these proton pairs (A5 C2H–H3-1, 0.54 nm; A6 C2H–H3-3, 0.43 nm) is too long to account for the intensities of the observed cross peaks. Furthermore, this model does not account for the observed drug–drug C20 CH_2 to FH NOEs that are less than 0.35 nm apart experimentally, but are 1.1 nm apart in this model.

In model B (Figure 4B), the drugs were again arranged symmetrically in the minor groove with each pyrrole ring positioned between two base pairs to satisfy the drug H3 to adenine C2H NOEs. This model was rejected because it failed to explain the observed drug H3 to DNA C1′H NOEs. Specifically, NOEs are observed between H3-1 and either T7 or T9 C1′H and between H3-2 and T8 C1′H (all distances less than 0.3 nm), while in models generated by interactive docking, these distances (H3-1–T7 C1′H, 0.56 nm; H3-1–T9 C1′H, 0.58 nm; H3-2–T8 C1′H, 0.44 nm) are too long to account for the intensities of the observed cross peaks.

Because models A and B failed to explain the observed NOEs, we considered a third model in which each drug was able to occupy either a 5′-AATT-3′ or a 5′-ATTT-3′ site, related by shifting the drug on the DNA sequence by one base pair. In this model, each of the drug pyrrole rings was positioned opposite a DNA base ring, which, depending on the site occupied, places the H3 protons adjacent to either of two A C2H and C1′H protons. This mode of binding, with the drug pyrrole rings in close contact with the DNA base pairs, has been observed in both 1:1 complexes of distamycin A[5b,7,8] and netropsin[9a,e–i] with A–T-rich sequences and in the 2:1 complex of distamycin A with d-(CGCAAATTGGC):d(GCCAATTTGCG).[7] It is necessary to assume, in order to account for the fact that only one set of drug and DNA resonances is observed, that the drug slides between the two sites at a rate that is near the fast-exchange limit. Such a sliding model accounts for the observed temperature-dependent line width of the aromatic and C1′H resonances (see the supplementary material). Together, these assumptions lead to three

(22) Distance upper limit based on comparison of drug–DNA cross-peak intensities with cytosine C5H–C6H cross-peak intensities (distance 0.245 nm).

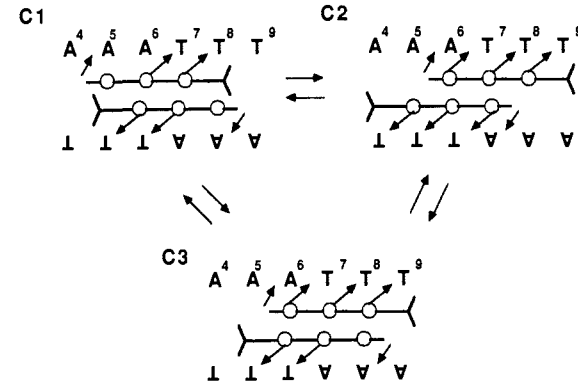

Figure 5. Schematic of the sliding model comprised of structures C1, C2, and C3. Circles represent drug pyrrole rings and attached H3 protons. NOEs are observed between each H3 proton (circle) and the adenine base to which it is adjacent, on either strand. NOEs from the DNA C1′H to drug FH and H3 protons are indicated by arrows.

different drug configurations within the A_3T_3 duplex denoted C1, C2, and C3 (Figure 5).

The close contacts predicted in the three structures C1, C2, and C3 account for all of the observed intermolecular NOEs. In C1, in which both drugs bind to AATT sites, the close contacts predicted between A5 C2H and H3-1 and between A6 C2H and both H3-2 and H3-3 account for three of the five observed H3–C2H NOEs. Similarly, the close contacts predicted between T7 C1′H and H3-2 and between T8 C1′H and H3-3 account for two of the five observed C1′H–H3 cross peaks. An NOE is also predicted between A6 C1′H and H3-1, which is not seen in the NOESY spectrum. As noted previously, however, the A6 C1′H resonance is broad at 20 °C, and the expected cross peak may be missing due to exchange broadening. NOEs observed between the drug formyl proton and A5 C1′H, between the drug C20 methylene protons and A5 C2H, and between the H3-2 and H3-3 protons of opposing drugs are also consistent with this mode of binding.

In C2, in which both drugs occupy ATTT binding sites, the close contacts predicted between A5 C2H and H3-3 and between A6 C2H and both H3-1 and H3-2 (also C1) account for the other H3–C2H NOEs observed in Figure 3. Similarly, the close contacts expected between T7 C1′H and H3-1, between T8 C1′H and H3-2, and between T9 C1′H and H3-3 account for the remaining C1′H–H3 NOEs. Furthermore, NOEs between the drug formyl proton and A6 C1′H, between the drug C20 methylene protons and A4 C2H, and between the drug H3-1 and H3-2 protons of opposing drugs are consistent with this mode of binding.

Finally, in C3, in which one drug occupies a 5′-AATT-3′ site and the other drug occupies a 5′-ATTT-3′ site, the drug–drug NOEs expected between the formyl and C20 methylene protons of opposing drugs, as seen in the previous 2:1 complex,[7b] and between the H3-1 and H3-3 protons are observed experimentally.

The analysis above shows that the three structures C1, C2, and C3, when taken together, are consistent with the observed stoichiometry, all of the observed NOEs, and the temperature-dependent exchange behavior. This interpretation is strengthened by our observation of a nonexchanging 2:1 complex with A_3T_2.[7b] Thus, we conclude that two types of binding sites, 5′-AATT-3′ and 5′-ATTT-3′, are occupied within the A_3T_3 sequence and that the complex is symmetric on the average due to rapid exchange of each drug among these two sites. A sliding model was also considered in a study on the binding of a netropsin analogue[12] to a DNA oligomer, but the model was rejected after comparison with the data. In all of the binding sites, the formyl end of the drug is directed toward the 5′-end of the strand with which it is in contact. Thus, the two positively charged propylamidinium groups are directed toward opposite ends of the helix, which minimizes any possible interaction between them and positions them to interact favorably with the DNA phosphates.[11b]

As mentioned previously, the three H3-H3 NOEs, each of which corresponds to a different model (Figure 5), differ in intensity.

Table III. Drug-DNA Hydrogen Bonds

drug amide proton	DNA proton	
	structure C1	structure C2
HN-1	A5 N3	A6 N3
HN-3	A6 N3	T7 O2
HN-5	T7 O2	T8 O2
HN-7	T8 O2	T9 O2

Since the intensity of a NOE cross peak is a function of both the time two protons are near one another and also the distance by which they are separated, these differences may reflect differences in the detailed interactions between the drug molecules in the three complexes or they may reflect differences in the populations of the three complexes in solution. In the latter case, which we favor, C2 (H3-1–H3-2 NOE) would be populated approximately twice that of C3 (H3-1–H3-3 NOE), while C3 would be populated approximately twice that of C1 (H3-2–H3-3 NOE).

On the basis of the distamycin A binding to the A_3T_3 duplex described here, as well as the very similar model for distamycin A binding to the A_3T_2 duplex,[7] we conclude that the sequence and orientational specificity of drug binding in the 2:1 mode is high. For the A_3T_2 duplex, one drug binds to an 5′-AATT-3′ site, while the other drug is in close contact with the sequence 5′-ATTT-3′ of the complementary strand. The addition of a sixth A–T base pair in A_3T_3 effectively creates two adjacent binding sites, both AATT and ATTT, on each strand of the helix. The pyrrole rings of the two drugs can all be adjacent to one another, as in C3, or they can be staggered, with only two of the three rings in close contact, as in C1 and C2. Moreover, we do not see any evidence for drug binding in the opposite orientation with the two positively charged propylamidinium groups in close contact. Furthermore, of the two possible antiparallel complexes (related by interchange of the drugs across the minor groove) only one is observed, indicating that the drugs are able to "read" the walls of the groove in considerable structural detail.

Models of C1 and C2 (Figure 6) were generated with a modified version of the AMBER[16] molecular mechanics program with semiquantitative intermolecular drug–drug and drug–DNA constraints derived from NOEs between these protons. The energy-minimized structures show hydrogen bonds between the drug amide protons and both the adenine N3 and thymine O2 atoms on the strand with which the drug is associated (Table III). Three-center hydrogen bonds seen in other drug–DNA complexes[5b,8,9e–g,10] are not possible in the 2:1 complex, because each drug is pushed against one wall of the minor groove.

Analysis of the energy-minimized structures also suggests that stacking interactions are important in stabilizing each complex. In C1, on one side the three pyrrole rings stack with A6, T7, and T8 sugar oxygen atoms, respectively. On the other side pyrrole ring one stacks with the positively charged amidinium group, while pyrrole rings two and three stack over the N7 and N5 amide groups of the opposing drug, respectively. For C2 and C3 the stacking interactions are similar to C1 and to those observed in the 2:1 distamycin A–A_3T_2 complex.[7b] Interactions between sugar oxygen atoms and aromatic rings have also been observed in 1:1 distamycin A–,[5b,8] netropsin–,[9e–g] and Hoechst 33258–DNA complexes,[10] as well as intramolecularly in Z-DNA.[23]

Our findings are quite different from those found in the single-crystal X-ray study of Wang et al.[8] with the same drug and DNA oligomer. They observe a single 1:1 binding mode for distamycin A with this duplex at a 1.1:1 drug:DNA ratio. NMR spectra of the A_3T_3 duplex with distamycin A added to this level, obtained both in phosphate buffer and in the buffer used in the X-ray study (supplementary material), revealed that the 2:1 complex was the primary species present. Thus, observation of only the 1:1 complex in the crystalline state appears to be due to selection by crystal-packing forces, rather it being the dominant form in the solution. In this regard, all of the A–T-rich oligomers so far crystallized with, and without, drug have narrow minor grooves.[8,9e–g,i,10,24] For instance, the minor-groove width of the A–T region of d(CGCGAATTCGCG)$_2$[24a] ranged from 0.32 to 0.40 nm (closest phosphate distance less two phosphate radii), while the minor-groove width of the A_3T_3 duplex with one bound drug was near 0.40 nm. If the van der Waals thickness of each drug is taken to be 0.34 nm, then the minor-groove width of the A_3T_3 duplex must expand at least 0.28 nm compared to the A_3T_3 duplex with one bound drug in order to accommodate both molecules. The fact that the 2:1 complex with the expanded minor groove was not crystallized, although it was present in the buffer, supports the notion of Wang et al.[9i] that a relatively narrow minor groove is, in fact, necessary for the crystallization of these oligomers in the $P2_12_12_1$ space group.

In addition to distamycin A, recent NMR studies of the G–C binding drugs actinomycin D[25] and chromomycin[26] have shown that these drugs are capable of binding as dimers to their respective oligomers and expand the minor groove along their binding sites. Additionally, an analogue of distamycin A with fluoromethylene

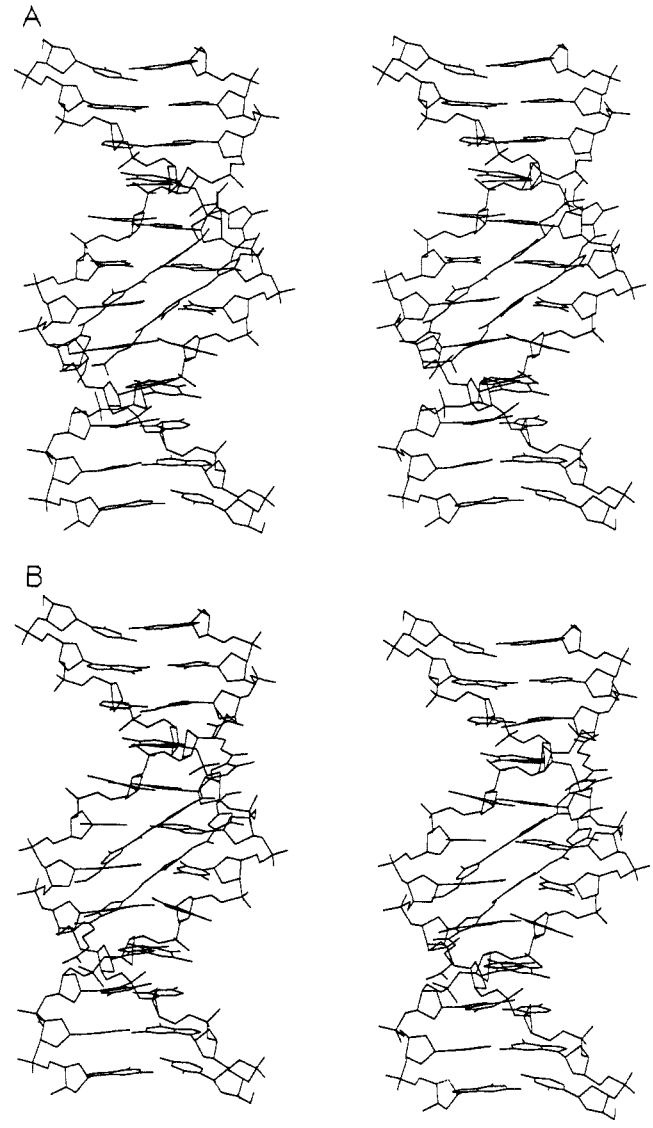

Figure 6. Stereodrawings of structures C1 (A) and C2 (B) obtained by energy refinement with semiquantitative distance constraints derived from NOESY spectra (see text).

(23) Wang, A. H.-J.; Quigley, G. J.; Kolpak, F. J.; Crawford, J. L.; van Boom, J. H.; van der Marel, G.; Rich, A. *Nature (London)* **1979**, *282*, 680–686.

(24) (a) Fratini, A. V.; Kopka, M. L.; Drew, H. R.; Dickerson, R. E. *J. Biol. Chem.* **1982**, *257*, 14686–14707. (b) Nelson, H. C. M.; Finch, J. T.; Luisi, B. F.; Klug, A. *Nature (London)* **1987**, *330*, 221–226.

(25) Scott, E. V.; Zon, G.; Marzilli, L. G.; Wilson, W. D. *Biochemistry* **1988**, *27*, 7940–7951.

(26) Gao, X.; Patel, D. J. *Biochemistry* **1989**, *28*, 751–762.

groups linking pyrrole rings has been observed to also bind in the minor groove,[27] although the detailed structure of this complex is not yet known and the affinity is relatively low. The width of these groups is similar to the stacked distamycins. These observations show that the phosphate backbone of both G–C- and A–T-rich sequences can distort significantly to accommodate ligands. In this regard, it is interesting to note that the 2:1 complex forms more easily relative to the one-drug complex when a G–C base pair (A_3T_2G) is replaced with an A–T base pair (A_3T_3). This may be due to differences in the details of the stacking interactions in C1 and C2 relative to C3 and the 2:1 A_3T_2 complex.[7] Another possibility is that the flanking G–C base pairs behave differently than the A–T base pairs with regard to allowable backbone conformational changes, hindering formation of the 2:1 complex in A_3T_2. Helix distortions have also been noted in several protein–DNA complexes.[28] The degree to which A–T and G–C base pairs alter the flexibility of the phosphate backbone and whether it is a factor in sequence-specific protein recognition remains to be determined.

Our results may have implications for other studies as well. Most footprinting and affinity cleaving studies have been conducted at relatively low drug concentrations when compared to the number of drug binding sites. However, in a DNase I footprinting study, the relative concentration of distamycin A was high enough that 2:1 complex formation may need consideration.[6] The 2:1 binding mode may also be of consequence in calorimetric[4] and other physical studies conducted at high drug/DNA ratios.

The sequence and orientational specificity seen in the 2:1 distamycin A–DNA complexes have implications for the design of new drugs and sequence-specific probes. As discussed previously,[7b] it may be possible to design molecules that, instead of interacting with both strands of the DNA, interact with one strand of the duplex and another drug molecule (or another part of the same drug) in a sequence-specific manner. Interactions that stabilize the present 2:1 complex and that should be considered in the design of such molecules include drug–drug and drug–DNA stacking, hydrogen bonding, and electrostatic forces.

(27) Wang, A. H.; Cottens, S.; Dervan, P. B.; Yesinowski, J. P.; van der Marel, G. A.; van Boom, J. H. *J. Biomolec. Struct. Dyn.* **1989**, *7*, 101–117.
(28) (a) Otwinowski, Z.; Schevitz, R. W.; Zhang, R.-G.; Lawson, C. L.; Joachimiak, A.; Marmorstein, R. Q.; Luisi, B. R.; Sigler, P. B. *Nature (London)* **1988**, *335*, 321–329. (b) Anderson, J. E.; Ptashne, M.; Harrison, S. C. *Nature (London)* **1987**, *326*, 846–852. (c) McClarin, J. A.; Frederick, C. A.; Wang, B.-C.; Greene, P.; Boyer, H. W.; Grable, J.; Rosenberg, J. M. *Science* **1986**, *234*, 1526–1541.

Conclusions

Both 1:1 and 2:1 binding modes have been observed for the binding of distamycin A with the sequence d-(CGCAAATTTGCG)$_2$, in contrast to the crystallographic result of Wang et al.[8] in which only a one-drug binding mode was evident. The data obtained on the 2:1 complex are consistent with a model in which each drug slides between 5′-AATT-3′ and 5′-ATTT-3′ binding sites associated with each strand of the duplex at a rate that is fast on the NMR time scale. Modeling of the 2:1 complexes indicates that electrostatic interactions, hydrogen bonds, and both drug–drug and drug–DNA stacking interactions are important in stabilizing the complex. Furthermore, binding two distamycin A molecules must expand the minor groove relative to what is seen in the X-ray study of the 1:1 distamycin A–A_3T_3 complex.[8] Our findings, in conjunction with those on actinomycin D[25] and chromomycin[26] that expand the minor groove of G–C regions and P1–F_4S–P1[27] that expands the minor groove of A–T-rich regions, suggest that the phosphate backbone of both A–T and G–C regions can be distorted to accommodate ligands. Whether the flexibility seen here is strongly sequence dependent and is important in sequence-specific recognition by proteins remains to be determined. It also remains to be seen whether the characteristics of the 2:1 complex can be exploited in the design of new sequence-specific recognition complexes.

Acknowledgment. We greatly appreciate the help of D. Koh with DNA synthesis. This work was supported by the National Institute of Health through the University of California—Berkeley Biological Research Support Grant program and equipment grants from the Department of Energy University Research Instrumentation program (DE F605 86ER75281) and the National Science Foundation (DMB 8609035).

Registry No. d(CGCAAATTTGCG)$_2$, 112139-33-0; distamycin A, 636-47-5.

Supplementary Material Available: Figure S1, an expansion of the aromatic to C1′H region of a NOESY spectrum of the free A_3T_3 duplex showing sequential connectivities, Figure S2, an expansion of the aromatic to C2′H/C2″H/CH_3 region of the NOESY spectrum acquired at 50 °C showing sequential connectivities of these protons, Figure S3, temperature dependence of aromatic and C1′H regions of the 2:1 complex spectrum, Figure S4, one-dimensional NOEs of imino protons used in assignments, Figure S5, comparison of aromatic and C1′H regions of 1S spectra in phosphate and crystallization buffers (5 pages). Ordering information is given on any current masthead page.